

## Toroidal curvature induced screening of external fields by a resistive plasma response

Yueqiang Liu, J. W. Connor, S. C. Cowley, C. J. Ham, R. J. Hastie et al.

Citation: *Phys. Plasmas* **19**, 072509 (2012); doi: 10.1063/1.4739062

View online: <http://dx.doi.org/10.1063/1.4739062>

View Table of Contents: <http://pop.aip.org/resource/1/PHPAEN/v19/i7>

Published by the [American Institute of Physics](#).

---

### Related Articles

Properties of convective cells generated in magnetized toroidal plasmas

*Phys. Plasmas* **19**, 082304 (2012)

Three-dimensional numerical investigation of electron transport with rotating spoke in a cylindrical anode layer Hall plasma accelerator

*Phys. Plasmas* **19**, 073519 (2012)

Physical characteristics of gliding arc discharge plasma generated in a laval nozzle

*Phys. Plasmas* **19**, 072122 (2012)

Electrostatic transport in L-mode scrape-off layer plasmas in the Tore Supra tokamak. I. Particle balance

*Phys. Plasmas* **19**, 072313 (2012)

Zonal flow triggers the L-H transition in the Experimental Advanced Superconducting Tokamak

*Phys. Plasmas* **19**, 072311 (2012)

---

### Additional information on Phys. Plasmas

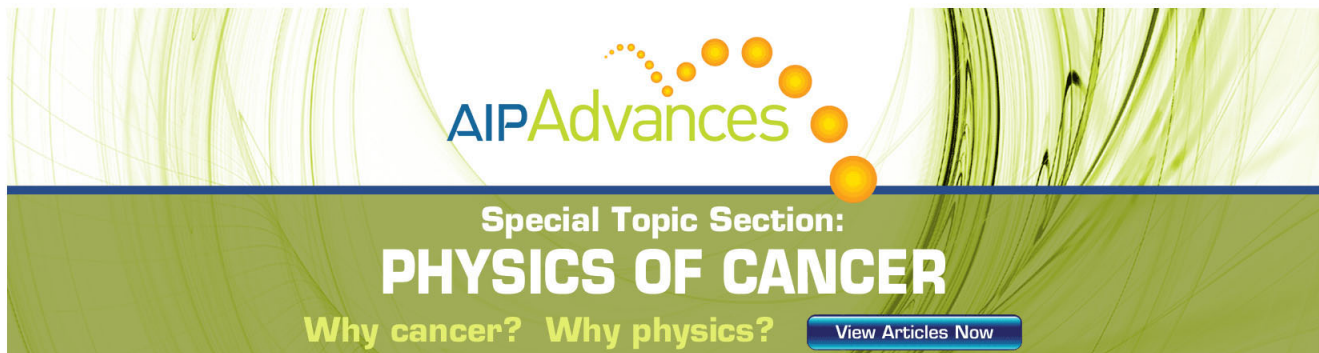
Journal Homepage: <http://pop.aip.org/>

Journal Information: [http://pop.aip.org/about/about\\_the\\_journal](http://pop.aip.org/about/about_the_journal)

Top downloads: [http://pop.aip.org/features/most\\_downloaded](http://pop.aip.org/features/most_downloaded)

Information for Authors: <http://pop.aip.org/authors>

## ADVERTISEMENT



**AIP Advances**

Special Topic Section:  
**PHYSICS OF CANCER**

Why cancer? Why physics? [View Articles Now](#)

# Toroidal curvature induced screening of external fields by a resistive plasma response

Yueqiang Liu,<sup>a)</sup> J. W. Connor, S. C. Cowley, C. J. Ham, R. J. Hastie, and T. C. Hender  
*Euratom/CCFE Fusion Association, Culham Science Centre, Abingdon OX14 3DB, United Kingdom*

(Received 28 May 2012; accepted 29 June 2012; published online 20 July 2012)

Within the single fluid theory for a toroidal, resistive plasma, the favorable average curvature effect [Glasser *et al.*, *Phys. Fluids* **18**, 875 (1975)], which is responsible for the strong stabilization of the classical tearing mode at finite pressure, can also introduce a strong screening effect to the externally applied resonant magnetic field. Contrary to conventional understanding, this screening, occurring at slow plasma rotation, is enhanced when *decreasing* the plasma flow speed. The plasma rotation frequency, below which this screening effect is observed, depends on the plasma pressure and resistivity. For the simple toroidal case considered here, the toroidal rotation frequency has to be below  $\sim 10^{-5}\omega_A$ , with  $\omega_A$  being the Alfvén frequency. In addition, the same curvature effect leads to enhanced toroidal coupling of poloidal Fourier harmonics inside the resistive layer, as well as reversing the sign of the electromagnetic torque at slow plasma flow. [<http://dx.doi.org/10.1063/1.4739062>]

## I. INTRODUCTION

The role of the plasma response to external non-axisymmetric magnetic fields in tokamaks has become increasingly important in view of the mitigation of edge localized modes (ELMs) using resonant magnetic perturbations (RMP),<sup>1–4</sup> the resonant field amplification effect in high pressure plasmas,<sup>5,6</sup> as well as (dynamic) error field correction.<sup>7</sup> While some of the external fields are intentionally applied for a good purpose (e.g., ELM mitigation using RMP fields), the others are often unintended and not desirable, since they degrade the plasma performance in terms of both macroscopic stability and confinement.

The theory of the plasma response to external fields has been extensively investigated, from early work, mostly in cylindrical geometry,<sup>8,9</sup> to recent work in both cylindrical<sup>10,11</sup> and toroidal geometry.<sup>12,13</sup>

While cylindrical theory is often useful in understanding the linear and non-linear,<sup>10</sup> as well as kinetic<sup>11</sup> physics associated with the plasma response, it sometimes leads to qualitatively different results from the toroidal theory prediction. A typical example is the response of a resonant harmonic ( $m, n$ ), with the poloidal harmonic number  $m$  and the toroidal harmonic number  $n$ , when the corresponding rational surface  $q = m/n$  ( $q$  is the safety factor) is located inside the plasma. In cases where a strong screening effect occurs, e.g., due to an ideal plasma response, or a fast plasma flow, the cylindrical theory would predict a vanishing resonant field on the inner side of the rational surface (where  $q < m/n$  for a monotonically increasing  $q$ -profile). Toroidal theory, on the other hand, predicts a finite amplitude of the resonant harmonic on the inner side of the rational surface, even though the field is perfectly shielded at the radial position of the rational surface. This is due to the toroidal coupling of the resonant harmonic to non-resonant harmonics, which can freely penetrate through

the rational surface. Sometimes, particularly for tight aspect ratio plasmas, the coupling can be so strong that the peak amplitude of the resonant harmonic exceeds that of the vacuum field.<sup>12,13</sup> In this work, we report another example where the toroidal effect plays an essential role in the plasma response. We consider a slowly rotating plasma, and numerically find a regime in the resistive plasma response, where decreasing the toroidal rotation frequency leads to an enhanced response of the resonant harmonic at the corresponding rational surface. The screening effect in this case comes from the same term in the toroidal tearing mode (TM) theory<sup>14</sup> which is responsible for the TM stabilization, resulting from the favorable average magnetic field curvature in a torus. We use the MARS-F code<sup>15</sup> to compute the plasma response. The code solves for the linear response of the plasma to a given external field, with a prescribed (fixed) plasma toroidal rotation. The external field is generated by currents located in the vacuum region. The combined MHD-vacuum-coil equations are solved together in MARS-F. One can refer to Ref. 12 for details of the MARS-F formulation when applied to the plasma response computations.

For the purpose of clarifying the physics, we assume simple toroidal equilibria as described in Sec. II. Section III reports the MARS-F results of the finite pressure gradient induced screening at slow plasma flow. This numerical finding is analytically explained in Sec. IV. The analytic understanding helps to design a new approach for computing the tearing index for a toroidal plasma, as demonstrated in Sec. V. Section VI reports additional effects associated with the favorable average curvature term, such as the enhancement of the toroidal coupling, as well as the sign reversal of the electromagnetic  $\mathbf{j} \times \mathbf{b}$  torque at slow plasma flow. Section VII draws conclusion and discussion.

## II. EQUILIBRIUM

We consider two toroidal equilibria—one with vanishing plasma pressure, and the other with a finite pressure—both having the same parabolic (surface-averaged) toroidal current

<sup>a)</sup>Author to whom correspondence should be addressed. Electronic mail: yueqiang.liu@ccfe.ac.uk.

density profile  $\langle J_\phi \rangle_{\text{surf}} = J_0(1 - s^2)$ , where  $s \equiv \sqrt{\psi_n}$ , and  $\psi_n$  is the normalized poloidal flux, with  $\psi_n = 0$  at the magnetic axis, and  $\psi_n = 1$  at the plasma boundary. The current amplitude  $J_0$  is eventually determined by choosing the safety factor  $q$  at the magnetic axis or at the plasma edge. The plasma has a large aspect ratio of 10 and a circular cross section. We choose the on-axis  $q$ -value to be  $q_0 = 1.05$ . The edge  $q$ -value is  $q_a = 2.46$  for the pressure-less equilibrium, and  $q_a = 2.62$  for the finite pressure equilibrium, which has a normalized beta value of  $\beta_N \equiv \beta[\%]a[m]B_0[T]/I_p[MA] = 1.60$ , where  $\beta = \langle P \rangle / (B_0^2 / 2\mu_0)$  is the ratio of the volume averaged plasma pressure to the magnetic pressure,  $a$  the minor radius of the plasma boundary,  $B_0$  the vacuum toroidal field strength at the magnetic axis, and  $I_p$  the total plasma current. The radial profiles of the safety factor and the equilibrium pressure are plotted in Fig. 1.

The reason for considering a large aspect ratio plasma is to allow an easy analytic interpretation of the numerical

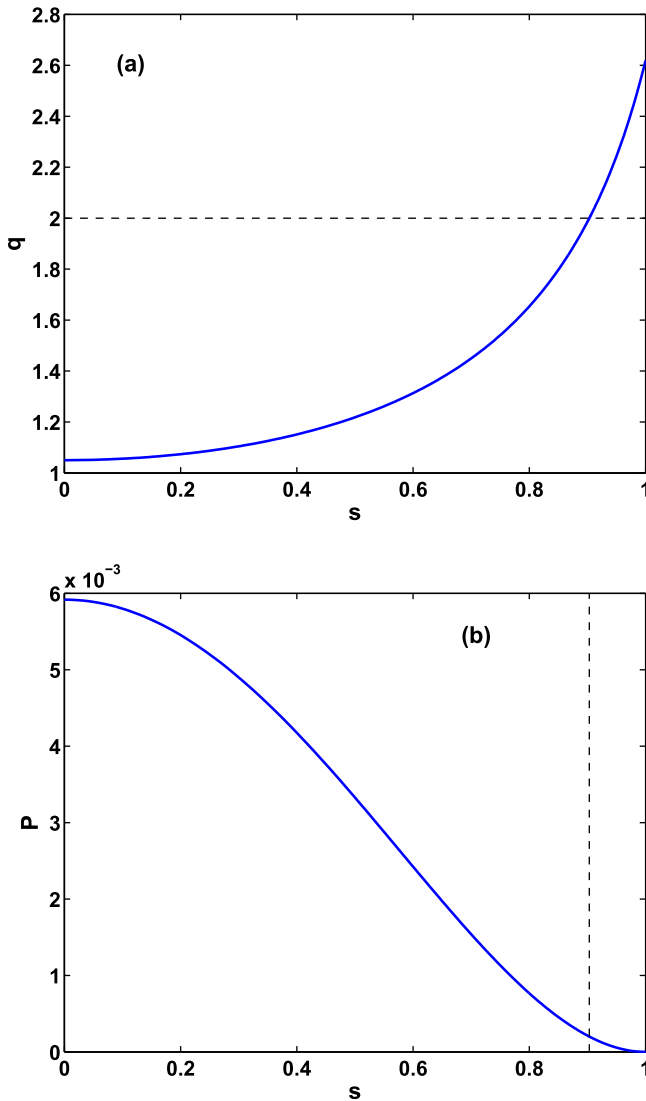


FIG. 1. Radial profiles of (a) safety factor  $q$ , and (b) equilibrium pressure, for a large aspect ratio toroidal plasma with circular cross section. The pressure is normalized by  $B_0^2/\mu_0$ . The radial coordinate  $s \equiv \sqrt{\psi_n}$  is defined via the normalized poloidal flux  $\psi_n$ . The vertical dashed line in (b) indicates the radial location of the  $q = 2$  rational surface.

results. As we will show in this work, a large aspect ratio theory not only confirms the qualitatively new features found by MARS-F runs but also gives a quantitative agreement with the computational results, thus confirming the correctness of the numerical procedures.

We shall consider the resistive plasma response to a  $n = 1$  external magnetic field, in the presence of an ideally conducting wall located at a minor radius of  $1.4a$ . Only one rational surface, with  $q = 2$ , is present inside the plasma for this field configuration.

### III. NUMERICAL COMPUTATION OF THE PLASMA RESPONSE

Figure 2 shows the MARS-F computed resistive plasma response to an external magnetic field perturbation produced by coils located near the outboard mid-plane at the minor radius of  $1.2a$ . The exact coil geometry is not important to observe the effects reported in the figure. The plasma response is measured by the ratio of the amplitude of the resonant harmonic of the total response field (including the field produced by both coil currents and the perturbed plasma currents), at the corresponding rational surface location, to that of the vacuum field. We scan the toroidal rotation frequency of the plasma. For simplicity, a uniform plasma flow profile in minor radius is assumed, characterized by an angular frequency  $\Omega$ . We also vary the magnetic Lundquist number  $S \equiv \tau_R/\tau_A$ , where  $\tau_A = R_0\sqrt{\mu_0\rho}/B_0$ ,  $\tau_R = a^2/\eta$ .  $R_0$  and  $a$  are the major and minor radii of the plasma, respectively,  $\rho$  is the plasma density (a uniform radial profile is assumed for the plasma density in this work), and  $\eta$  is the plasma resistivity (a uniform radial profile is also assumed for  $\eta$ ).

At a finite plasma pressure ( $\beta_N = 1.6$  in our case), two regimes of rotational screening of the resonant harmonic ( $m = 2$  in our case) are identified. The first regime occurs at very slow toroidal rotation speed, with  $\Omega < \sim 10^{-5}\omega_A$ . In this regime, the (total) plasma response increases with increasing toroidal flow speed, following approximately a

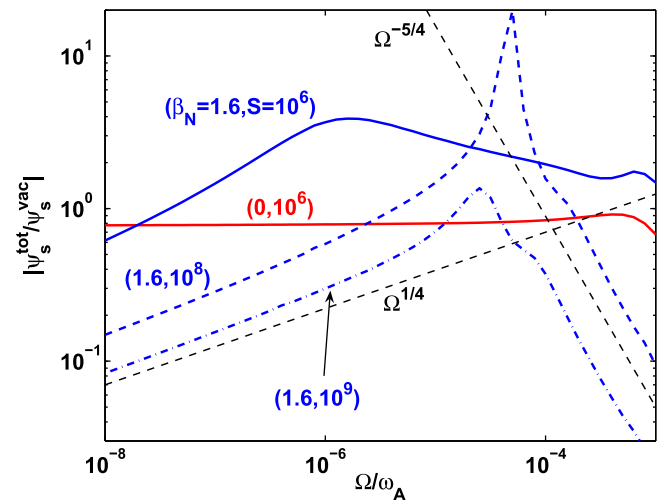


FIG. 2. Computed resistive plasma response for the  $m = 2$  resonant harmonic at slow plasma rotation. At finite pressure ( $\beta_N = 1.6$ ), two regimes of rotational screening of the plasma response are identified, with opposite trends. The two dashed straight lines indicate analytic scaling laws.

scaling law of  $\Omega^{1/4}$ . In other words, the plasma flow does *not* provide a screening effect of the external field but tends to amplify the field instead. This trend (as well as the scaling law) does not depend on the plasma resistivity. We shall call this regime the GGJ-regime, for reasons to be clarified later on.

When the plasma rotation frequency exceeds a certain level (about  $10^{-4}\omega_A$  in our example), the flow does start to provide a screening effect on the external field, i.e., an increase of the rotation speed leads to a reduced (total) plasma response for the resonant harmonic, following an approximate scaling law of  $\Omega^{-5/4}$ . This second regime corresponds to the resistive-inertial (RI) regime of the plasma response.<sup>9</sup> The transition region between the GGJ-regime and the RI-regime depends on the plasma resistivity and pressure. This dependence will be clarified in Sec. IV, when an analytic interpretation of the numerical results is given.

It is interesting to notice that the plasma response peaks in an intermediate region between the GGJ-regime and the RI-regime. In particular, at  $S = 10^8$  and  $\Omega = 5 \times 10^{-5}\omega_A$ , the plasma response amplitude is about 20 times higher than the vacuum field—a significant amplification of the external resonant field by the plasma response. This strong amplification occurs when the tearing mode is close to marginal stability, and the plasma rotation speed matches the natural frequency of the mode (see Fig. 6 in later discussions).

We note that the GGJ-regime occurs only at a finite plasma pressure. More precisely, it occurs only when the local pressure gradient at rational surface is finite, which is the case in our example. With vanishing pressure (and hence local pressure gradient), the plasma response saturates at a constant level as the flow speed is reduced. One such example is shown in Fig. 2.

The reduction of the plasma response (with decreasing rotation frequency) in the GGJ-regime is associated with the generation of a finite amplitude perturbed  $m/n = 2/1$  plasma current at the rational surface. Figure 3(a) shows one example of the MARS-F computed poloidal component of the  $m/n = 2/1$  current near the  $q = 2$  rational surface. The  $m = 2$  is the dominant harmonic for the poloidal component of the perturbed currents. Note that these perturbed plasma currents, induced by the plasma response to external fields, are highly localized along the minor radius, with an appreciable amplitude observed only within the resistive layer. A finite amount of the net perturbed current (across the layer) is responsible for providing the eventual screening effect at very slow rotation. A significant amount of the perturbed toroidal current is also observed. This current has large sideband poloidal harmonics, which are balanced by the perturbed radial current across the layer (to satisfy the divergence-free condition for the full current).

At vanishing plasma pressure, the  $2/1$  perturbed current has odd symmetry across the rational surface, as shown by Fig. 3(b) for the poloidal component. The toroidal component, not shown here, also has an oddly symmetric, predominant  $2/1$  harmonic. The cancellation effect between perturbed currents, flowing in opposite directions on either sides of the rational surface, leads to reduced screening for the plasma with vanishing pressure.

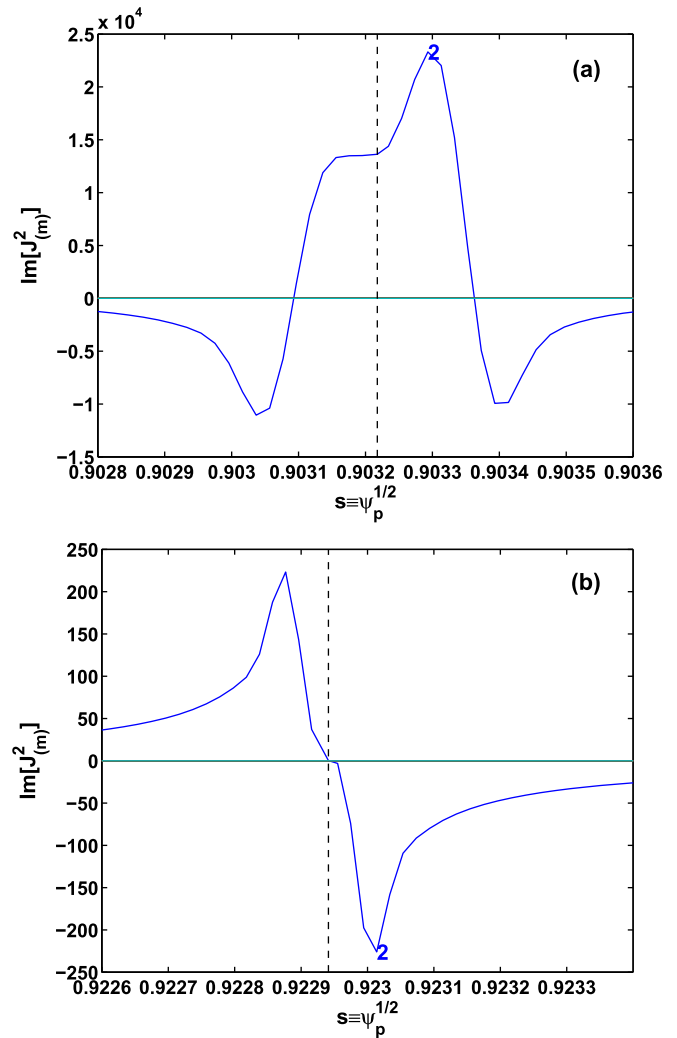


FIG. 3. Comparison of the poloidal components of the  $m = 2$  plasma response currents near the  $q = 2$  rational surface, at (a) a finite plasma pressure  $\beta_N = 1.6$  and (b) vanishing plasma pressure. The same plasma resistivity and rotation frequency are assumed, with  $S = 10^9$  and  $\Omega = 10^{-8}\omega_A$ . Note that the range of the x-axis covers only 0.08% of the whole plasma minor radius in each case.

#### IV. ANALYTIC INTERPRETATION

We propose an analytic interpretation of the numerically computed plasma response results shown above, based on an earlier work by Fitzpatrick and Hender.<sup>8</sup> In the presence of a static external magnetic field  $\psi_{\text{vac}}$  ( $\psi$  here denotes the poloidal flux of the perturbed field), the full plasma response can be separately considered in two regions: the internal layer region near rational surfaces, where the plasma resistivity and inertia are important, and the external ideal region, where the plasma resistivity and inertia can be neglected. According to Ref. 8, the external (ideal) response  $\psi_{\text{ext}}$  can be decomposed into two parts: the conventional solution  $\psi_0$  of the Newcomb equation in the absence of external field (with appropriate boundary conditions at the plasma center and at an ideal wall or infinity), and the ideal plasma response  $\psi_1$  in the presence of the external field (i.e., with the boundary condition  $\psi_1(r_s) = 0$ ). For a pressure-less plasma, the external response  $\psi_{\text{ext}}$  experiences a jump in its derivative with respect to the minor radius, on crossing the rational surface.



This gives an external tearing index  $\Delta'_{\text{ext}}$  in the presence of the external field, to be matched to the internal  $\Delta'_{\text{int}}$  from the layer solution.

The external  $\Delta'_{\text{ext}}$  is calculated as

$$\Delta'_{\text{ext}} \equiv \frac{[\psi'_{\text{ext}}]_{r_s}}{\psi_{\text{ext}}(r_s)} = \frac{[\psi'_0]_{r_s} + [\psi'_1]_{r_s}}{\psi_0(r_s)} = \Delta'_0 + \frac{[\psi'_1]_{r_s}}{\psi_0(r_s)}, \quad (1)$$

where  $[\cdot]$  denotes the jump across the rational surface, and  $\psi_{\text{ext}}(r_s) = \psi_0(r_s)$  represents the fully reconnected flux.  $\Delta'_0$ , by definition, is the tearing index in the absence of external fields. For a linear response,  $\psi_1$ , and hence  $[\psi'_1]_{r_s}$ , is proportional to the external field amplitude

$$[\psi'_1]_{r_s} = \alpha \psi_{\text{vac}}(r_s). \quad (2)$$

Equations (1) and (2) yield

$$\frac{\psi_{\text{ext}}(r_s)}{\psi_{\text{vac}}(r_s)} = \frac{\alpha}{-\Delta'_0 + \Delta'_{\text{ext}}}.$$

For a straight cylinder with circular cross section, the coefficient  $\alpha$  is calculated to be  $\alpha = 2m$  (assuming vanishing plasma current outside the rational surface).<sup>8</sup> The matching condition between the external and the internal layer solutions,  $\Delta'_{\text{ext}} = \Delta'_{\text{int}}$ , finally leads to the following expression for the plasma response:

$$\frac{\psi_{\text{ext}}(r_s)}{\psi_{\text{vac}}(r_s)} = \frac{\alpha}{-\Delta'_0 + \Delta'_{\text{int}}}. \quad (3)$$

Note that  $\Delta'_{\text{int}}$  is calculated by solving the inner layer equations,<sup>14,16</sup> and  $\Delta'_{\text{int}}$  is generally a function of the tearing mode (complex) frequency. For a large aspect ratio circular plasma with finite pressure,  $\Delta'_{\text{int}}$  is calculated as<sup>17</sup>

$$\Delta'_{\text{int}} = 2.12A(\gamma\tau_A)^{5/4} \left[ 1 - \frac{\pi}{4} D_R B (\gamma\tau_A)^{-3/2} \right], \quad (4)$$

$$A \equiv \left( \frac{nq'}{q} \right)^{-1/2} (1 + 2q^2)^{1/4} S^{3/4}, \quad (5)$$

$$B \equiv \left( \frac{nq'}{q} \right) (1 + 2q^2)^{-1/2} S^{-1/2},$$

where  $\gamma$  is the tearing mode growth rate (generally a complex number). The prime is defined with respect to the minor radius  $r$ :  $q' = dq/dr$ .  $D_R$  is the resistive interchange index that can be analytically calculated for a large aspect ratio circular plasma.<sup>17</sup> All the equilibrium quantities are defined at the rational surface  $r_s$ . Note that Eq. (4) is the large aspect ratio version of a more generic expression, Eq. (88) from Ref. 14.

The term associated with  $D_R$  is the key factor responsible for the screening of the plasma response at very slow rotation (the GGJ-regime), reported in the above numerical results. This term, first introduced by Glasser, Greene, and Johnson (GGJ)<sup>14</sup> for a general torus, originates from the favorable average magnetic curvature in the layer region. A similar term, in the constant- $\psi$  approximation, was also derived for a resistive pinch,<sup>16</sup> where a stabilizing effect on the TM was shown when the plasma pressure decreases outward. This screening

effect disappears as the local radial gradient of the plasma equilibrium pressure vanishes at the rational surface.  $[D_R]$  is roughly proportional to  $dP_{\text{eq}}/dr|_{r_s}$  and is normally a small negative number (resistive interchange stable).  $D_R = -0.04$  for our numerical equilibrium with  $\beta_N = 1.6$ .]

In the case of vanishing  $D_R$  (in our equilibrium with  $\beta_N = 0$ ), it can easily be shown that Eq. (4) precisely converts to the plasma response model derived in Ref. 9, for the resistive-inertial regime, on replacing  $\gamma$  by  $i\Omega$  in (4), representing the Doppler shifted mode frequency due to the plasma rotation  $\Omega$ . In this regime, the plasma response scales as  $\Omega^{-5/4}$  at sufficiently large rotation frequency, confirming our numerical findings. Also, the plasma response saturates to a constant value as plasma rotation vanishes.

In the case of a finite  $D_R$  value, the GGJ-term significantly modifies the inner layer response, and hence  $\Delta'_{\text{int}}$ . Equation (3), combined with (4), predicts a different scaling of the plasma response at very slow rotation:  $\psi_{\text{ext}}(r_s) \propto \Omega^{1/4}$ . This again confirms the numerical results, showing that the GGJ-term plays a screening effect on the external field at very slow plasma rotation.

The analytic scalings in (4) and (5) suggest that the rotation has to be smaller than  $\min\{S^{-1/3}|D_R|^{2/3}, S|D_R/\Delta'_0|^{1/4}\}$  (assuming the magnetic shear at the rational surface to be of order 1 quantity), in order to observe the GGJ-regime. For typical plasma parameters,  $S^{-1/3}|D_R|^{2/3} < S|D_R/\Delta'_0|^{1/4}$ , and hence the GGJ-term induced screening occurs when the toroidal rotation frequency, normalized by the central Alfvén frequency, is below  $\Omega_{\text{GGJ}} \sim S^{-1/3}|D_R|^{2/3}$ . For the large aspect ratio plasma considered here,  $\Omega_{\text{GGJ}} \sim 10^{-4}$  at  $S = 10^9$ , confirming the results shown in Fig. 2. However, for a tight aspect ratio plasma, the  $|D_R|$  can be one order of magnitude larger. If we are interested in the screening effect near the plasma edge region, the Lundquist number can be 2-3 orders of magnitude smaller than  $10^9$ . Therefore, the GGJ-term induced screening can be observed at much faster plasma flow.

## V. COMPUTING THE TEARING INDEX USING THE PLASMA RESPONSE

The expression (3) suggests a possible approach to computing the conventional tearing index  $\Delta'_0$  (in the absence of external fields) by computing the plasma response to external fields, provided that the inner  $\Delta'_{\text{int}}$  can be calculated in some way. For a generic toroidal equilibrium,  $\Delta'_{\text{int}}$  can be evaluated either using the analytic toroidal layer solution (Eq. (87) from Ref. 14), which is valid within certain limits, or a code such as DELTAR (Ref. 18) to numerically solve the toroidal resistive layer equations.

For our simple equilibria, we shall use Eq. (4) to evaluate  $\Delta'_{\text{int}}$ , and then use Eq. (3) to compute  $\Delta'_0$ , based on the MARS-F computed resistive plasma response  $\psi_{\text{ext}}/\psi_{\text{vac}}$  at the rational surface.

First, consider the equilibrium with vanishing pressure. Figure 4 shows the least-square fitting to the results of the MARS-F computed response (both amplitude and phase), using the analytic relation (3) combined with (4). The two unknowns  $\Delta'_0$  and  $\alpha$  are used as the fitting parameters. This yields  $\Delta'_0 = 7.73$  and  $\alpha = 6.25$ .

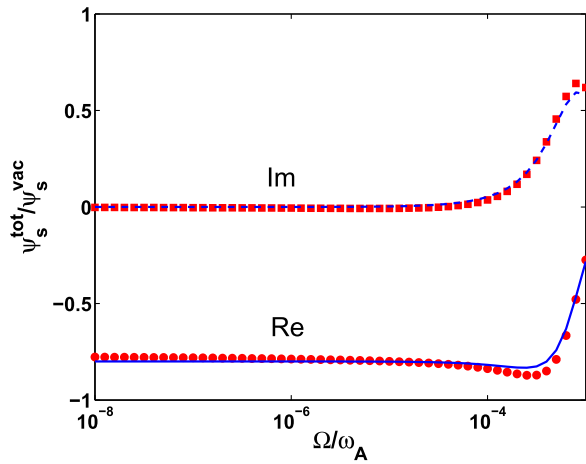


FIG. 4. The real and imaginary parts of the numerically computed plasma response (dots) and the least-square fits (lines) using the analytic relation (3), for a large aspect ratio equilibrium with vanishing plasma pressure. The plasma response is scanned versus the toroidal rotation frequency  $\Omega$ . The magnetic Lundquist number for the plasma is assumed to be  $S = 10^6$ .

Here, we make a remark on the plasma response computation, when the tearing mode is actually unstable (e.g.,  $\Delta'_0 > 0$  for the pressure-less case). There is of course no physically meaningful steady state response for an unstable plasma. However, numerically it is still possible to find the “steady-state” solution of an unstable system. This basically corresponds to finding the stationary point ( $\partial/\partial t = 0$ ) of an (unstable) system. The plasma response, computed in this sense, still contains the information of the (positive) poles of the system. A similar idea has been exploited in constructing plasma response models for feedback stabilization of unstable resistive wall modes.<sup>23</sup>

On the other hand, MARS-F can also solve for the tearing mode eigenvalue problem without the external fields, and with the same ideal wall condition at  $r = 1.4a$ . The computed tearing mode growth rates  $\gamma$  are then inserted into the dispersion relation (4) to yield  $\Delta'_{\text{int}}$ . This approach has been used previously.<sup>19,20</sup> In the absence of the external field,  $\Delta'_{\text{int}} = \Delta'_0$ , i.e., the conventional tearing index. The value of  $\Delta'_0$ , computed in this way, is not sensitive to the  $S$  number, as long as  $S$  is sufficiently large. For  $S = 10^8$ , MARS-F finds  $\Delta'_0 = 7.86$ , agreeing well with that of the plasma response computations.

We remark that the above TM growth rate method, based on the dispersion relation (4) (omitting the GGJ-term for the pressure-less plasma considered here), tends to significantly under-estimate  $\Delta'_0$  at  $S$ -values below  $10^6$ . For instance, the method yields  $\Delta'_0 = 6.19$  for  $S = 10^5$ . This is essentially due to the asymmetric radial distribution of the equilibrium current near the rational surface.<sup>21</sup> If the correction factor from Ref. 21 is taken into account,  $\Delta'_0$  can be recovered within a relative error of 5%, for  $S$ -values as low as  $10^3$ . For the results reported in this paper, we consider  $S \geq 10^6$ , this asymmetry correction factor is small.

For a pressure-less plasma, we have also devised a third method of computing  $\Delta'_0$ , based on the construction of large and small solutions for the outer region solution.<sup>22</sup> This third method, completely different from the response method and

the TM growth rate method reported here, gives  $\Delta'_0 = 7.71$  for our example, again within a good agreement with the other two methods.

We also tested the response method for a truly TM-stable, pressure-less plasma, with the same plasma shape and the same equilibrium current profile, but with elevated  $q$  values ( $q_0 = 3.1, q_a = 4.9$ ). In this case, the response method gives  $\Delta'_0 = -1.68$ , whilst the construction method gives  $\Delta'_0 = -1.66$ .

Next, we show an example of the response method applied to the finite pressure plasma, where a screening effect is observed in the slow rotation GGJ-regime. In this case, the least-square fit to the plasma response, shown in Fig. 5, yields  $\Delta'_0 = 31.37$ . The TM growth rate method, on the other hand, gives  $\Delta'_0 = 31.45$ .

For this equilibrium, the tearing mode is again unstable at low  $S$  values (e.g.,  $S = 10^6$ ). However, above a critical value of  $S_{\text{crit}} = 9.2 \times 10^7$ , the TM is stabilized by the GGJ-effect. The MARS-F computed TM eigenvalues, in the absence of the plasma flow, are plotted in the complex plane in Fig. 6. Evidently the computed plasma response, shown in Fig. 2, is for an unstable plasma at  $S = 10^6$ , and stable plasmas at  $S = 10^8$  and  $S = 10^9$ . We note that the tearing mode becomes marginally stable at  $S = S_{\text{crit}} = 9.2 \times 10^7$  for our equilibrium, with a natural frequency of the mode  $\omega_{\text{TM}} = 4.7 \times 10^{-5}\omega_A$  at the marginal stability. The maximal response amplitude, shown in Fig. 2 at  $S = 10^8, \Omega = 5 \times 10^5\omega_A$ , occurs as the tearing mode approaches the marginal stability and the plasma rotation speed matches the natural frequency of the mode. It is clear from Eq. (3) that the denominator from the right hand side approaches zero as the above two conditions are satisfied, and hence an infinitely large plasma response is expected in theory.

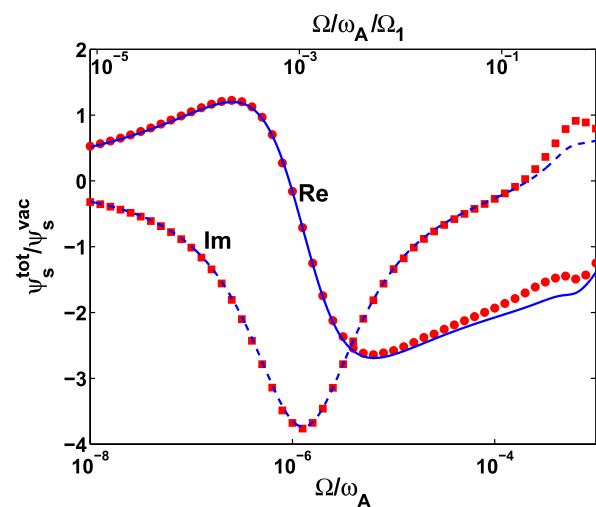


FIG. 5. The real and imaginary parts of the numerically computed plasma response (dots) and the least-square fits (lines) using the analytic relation (3), for a large aspect ratio equilibrium with finite plasma pressure ( $\beta_N = 1.6$ ). The plasma response is scanned versus the toroidal rotation frequency  $\Omega$ . The magnetic Lundquist number is assumed to be  $S = 10^6$ . The horizontal axis along the top of the figure is subject to an additional normalization factor of  $\Omega_1 \equiv S^{-1/3}|D_R|^{2/3}$ .

The computed TM eigenvalues, shown in Fig. 6, can be inserted into Eq. (4) to calculate  $\Delta'_{\text{int}}$ . We find that a numerical factor, of about 0.4 for the case considered here, needs to multiply the GGJ-term in Eq. (4), in order to obtain  $\Delta'_{\text{int}}$  with a minimal imaginary part (about 3.5% of the real part). [In the absence of the plasma flow,  $\Delta'_0$  from the ideal region is a real number. Consequently,  $\Delta'_{\text{int}}$  from the layer solution, which should match the outer solution, is also real despite the fact that the TM growth rate  $\gamma$  can be a complex number.] This numerical factor varies with the choice of plasma equilibria.

A close examination of the equilibrium parameters reveals that, for the finite pressure case considered here, the factor  $|GD_R|^{1/2} = 3.72 > 1$ , and hence the validity of the dispersion relation (4) is violated (the definition of the  $G$ -factor, as well as the  $H$ -factor mentioned below, is given in Refs. 14 and 17). In this case, another dispersion relation, Eq. (A9) from Ref. 14 and re-produced below for a large aspect ratio plasma, should be used instead

$$\Delta'_{\text{int}} = \frac{\pi}{2\tau} \left[ \left( \frac{nq'}{q} \right)^2 \frac{S^2}{1+2q^2} \right]^{1/6} Q^{5/4} \times \left\{ (aR_+ + b) \frac{\Gamma[(3-R_+)/4]}{\Gamma[(5-R_+)/4]} - (aR_- + b) \frac{\Gamma[(3-R_-)/4]}{\Gamma[(5-R_-)/4]} \right\}, \quad (6)$$

where  $Q \equiv \gamma\tau_A/Q_0$ ,  $Q_0 \equiv [(nq'/q)^2/(S(1+2q^2))]^{1/3}$ ,  $a \equiv 1 - D_R/Q^{3/2}$ ,  $b \equiv D_R/Q^{3/2} + CQ^{3/2} - (C - KD_R)D_R$ ,  $\tau \equiv [C^2Q^3 + 4(C - KD_R)D_R]^{1/2}$ ,  $R_{\pm} \equiv (-CQ^{3/2} \pm \tau)/2$ . All the equilibrium quantities, including the  $C$ ,  $K$  factors as calculated in Ref. 17, are evaluated at the rational surface.

The above dispersion relation (6) is valid for a vanishing  $H$ -factor (i.e., when the so-called constant- $\psi$  approximation holds). For our equilibrium,  $H=0.036$  is small. Indeed, inserting the MARS-F computed TM growth rates, shown in Fig. 6, into (6), we obtain  $\Delta'_{\text{int}}$  with a negligible imaginary part.

It was stated in the Appendix of Ref. 14 that Eq. (6) recovers (4) by a Taylor expansion of the gamma functions. We find that a more rigorous derivation (following the same gamma function expansion, but keeping the finite term which is proportional to  $|GD_R|$ ) results in an additional factor, such that Eq. (4) is modified to

$$\Delta'_{\text{int}} = 2.12(1+g)A(\gamma\tau_A)^{5/4} \left[ 1 - \frac{1}{1+g} \frac{\pi}{4} D_R B (\gamma\tau_A)^{-3/2} \right], \quad (7)$$

where  $g \simeq (\frac{\pi}{4} - 1)GD_R$ . The factors  $A$  and  $B$  are again defined by Eq. (5). For cases where  $|GD_R|^{1/2} > 1$  (but not too much larger than unity so that the Taylor expansion of the gamma functions in Eq. (6) still holds), the factor  $1/(1+g)$  can significantly deviate from unity. In fact for our example,  $1/(1+g) = 0.25$ , which is comparable to the value of 0.4 found numerically with MARS-F results. The agreement should become better

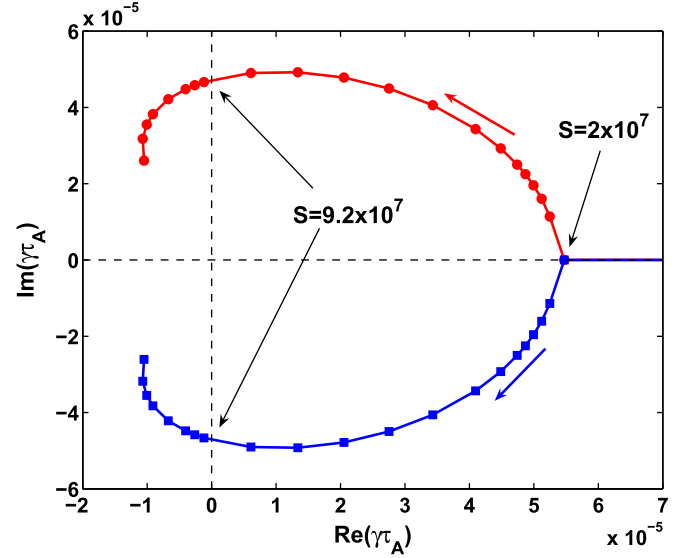


FIG. 6. The computed TM eigenvalues plotted in the complex plane, as the magnetic Lundquist number  $S$  varies, for a finite pressure, non-rotating resistive plasma. The point, where the real growth rate bifurcates into two (complex conjugate) branches, corresponds to  $S = 2 \times 10^7$ . The critical  $S$  value, for marginal stability of the TM, is  $S_{\text{crit}} = 9.2 \times 10^7$ .

on reducing the  $|GD_R|^{1/2}$  value. We checked another equilibrium, where the  $|GD_R|^{1/2}$  value is reduced to 0.38 by running MARS-F with the ratio of the specific heats  $\Gamma = 100$ . In this case, both analytic theory and the MARS-F results find a correction factor of  $1/(1+g) = 0.96$ .

We remark two important roles played by the correction factor  $1/(1+g)$ . First, it introduces the plasma compressibility into the TM dispersion relation, since  $g$  is inversely proportional to  $\Gamma$ . The plasma compressibility normally drops out of the TM dispersion relation (Eqs. (87) and (88) from Ref. 14) when it is treated as a higher order effect in the layer theory. Second, this correction factor is essential for producing real  $\Delta'_{\text{int}}$  from the computed (complex) TM growth rate.

## VI. OTHER EFFECTS ASSOCIATED WITH FINITE PLASMA PRESSURE

We report two additional effects associated with the GGJ term for finite pressure plasmas. The first is the enhanced toroidal coupling of poloidal Fourier harmonics in the layer region. This effect is illustrated in Fig. 7, where the eigenfunctions of unstable tearing modes, one with vanishing plasma pressure and the other with a finite plasma pressure ( $\beta_N = 0.71$ ), are compared in the layer region. These two plasmas have the same aspect ratio of 10, the same equilibrium current profile as described in Sec. II, and the same central safety factor  $q_0 = 1.05$ . The magnetic Lundquist number is also chosen to be the same,  $S = 10^6$ . An ideal wall, located at  $r = 1.4a$ , is assumed. The growth rate of the tearing mode at  $\beta_N = 0$  is  $\gamma\tau_A = 7.50 \times 10^{-4}$ . The growth rate at  $\beta_N = 0.71$  is  $\gamma\tau_A = 7.56 \times 10^{-5} + 5.33 \times 10^{-5}i$ . Note that the complex growth rate for the finite pressure case is due to the GGJ term. No plasma rotation is assumed in these computations.

Comparing figures (a,c) with (b,d), we observe that both the local plasma displacement and the perturbed parallel current density have an enriched poloidal spectrum at finite

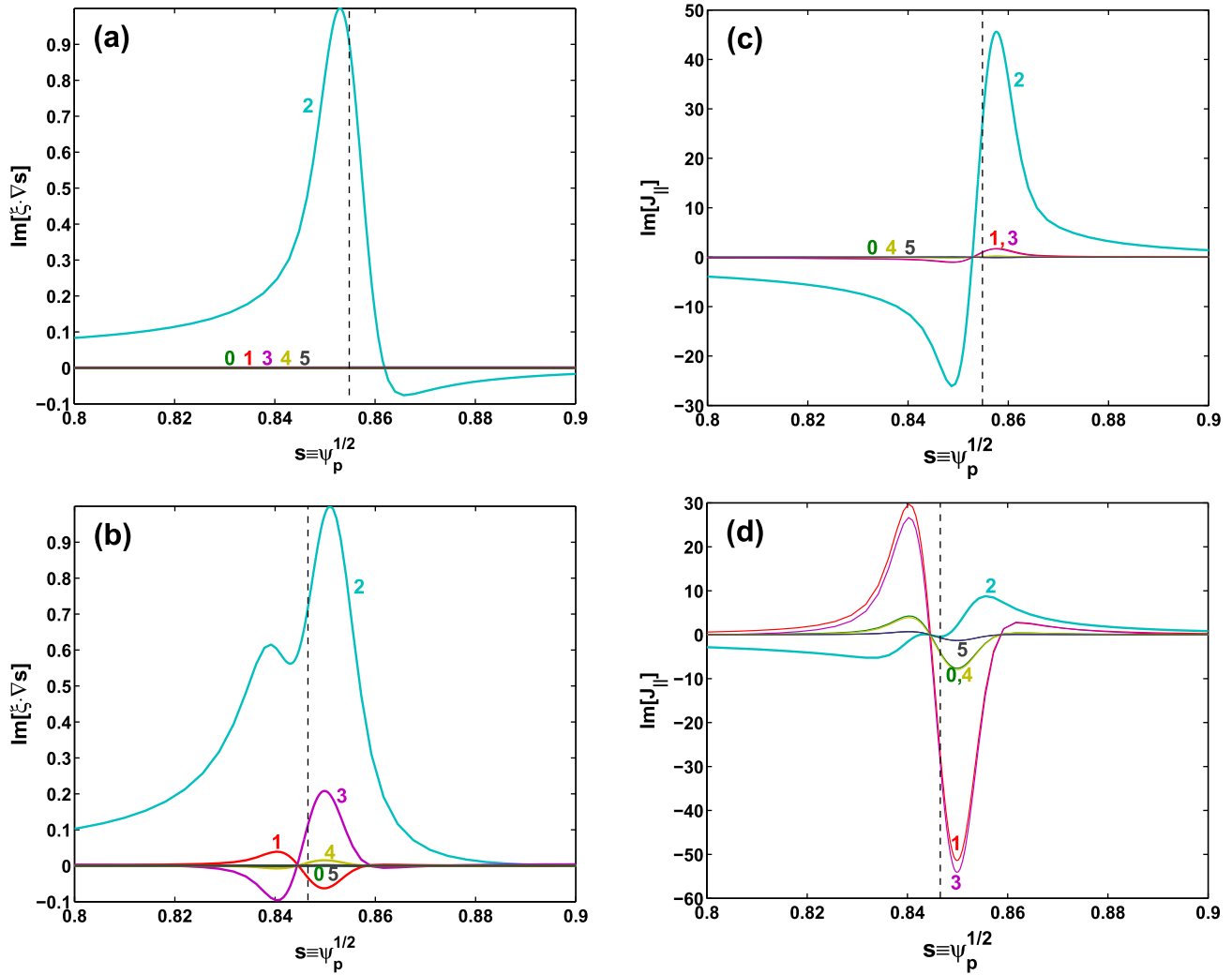


FIG. 7. Radial profiles of the poloidal Fourier harmonics for the plasma radial displacement (a, b) and perturbed parallel current density (c, d). Compared are the eigenfunctions of unstable tearing modes for the case with vanishing plasma pressure (a, c) and the case with a finite plasma pressure  $\beta_N = 0.71$  (b, d). The vertical dashed lines indicate the radial location of the  $q = 2$  rational surface. The Lundquist number is  $S = 10^6$  for both cases.

pressure. The  $m = 1, 3$  sideband harmonics, with respect to the  $m = 2$  resonant harmonic, have a much enhanced amplitude at finite pressure. This effect is even more pronounced for the parallel current density, where the secondary sidebands,  $m = 0, 4$ , also gain appreciable amplitudes, and where the amplitude of the resonant harmonic ( $m = 2$ ) actually becomes smaller than that of the non-resonant harmonics. The same observations hold for several other cases that we have considered.

The second interesting effect, associated with the finite pressure plasma response, is the electromagnetic torque produced on the (rotating) plasma by an external static field. Figure 8 shows one example, where the total toroidal  $\mathbf{j} \times \mathbf{b}$  torques, acting on the plasma column, are compared for the two equilibria described in Sec. II. The external field is produced by a dc-current (with the same current amplitude for the two cases) located at a minor radius of  $1.2a$ , in the presence of a perfectly conducting wall located at  $1.4a$ . The toroidal plasma rotation frequency  $\Omega$  is scanned.

The most interesting feature in the electromagnetic torque is the presence of a positive torque (i.e., in the same direction as the plasma flow), at very slow plasma rotation,

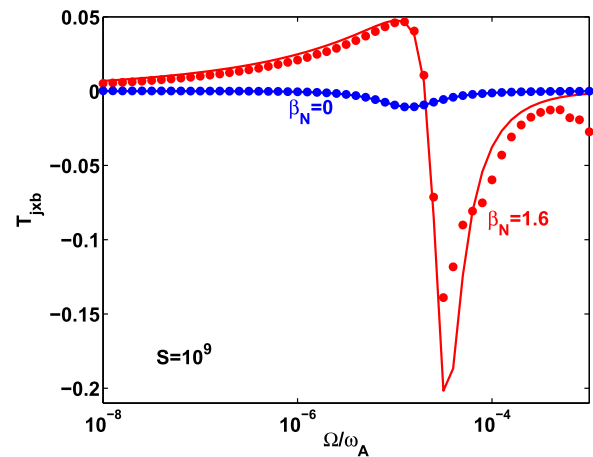


FIG. 8. Comparison of the computed total toroidal electromagnetic torque  $T_{\mathbf{j} \times \mathbf{b}}$  across the plasma column, induced by the response of a rotating resistive plasma to a static external field, produced by a coil current located at the minor radius  $r = 1.2a$ . Two plasmas, with the same Lundquist number  $S = 10^9$  but with different equilibrium pressures ( $\beta_N = 0$  and  $1.6$ , respectively), are compared. The MARS-F computed torques (dots) are also compared with the analytic estimates (lines).



due to the finite pressure plasma response. In fact, the total torque reverses sign at a certain rotation frequency, for the finite pressure plasma. No such reversal is obtained for the zero pressure case.

This torque reversal effect implies the existence of a finite steady state plasma rotation frequency, for a finite pressure plasma, even without invoking the finite plasma viscosity assumption. [The finite plasma viscosity is normally the force that balances the electromagnetic torque, in order to achieve a steady state plasma rotation<sup>9</sup>.]

Figure 8 also shows a significant amplification effect of the torque amplitude due to finite plasma pressure. This amplification is even stronger with increasing plasma resistivity.

The computed dependence of the toroidal torque on the plasma rotation frequency (dots in Fig. 8) is well approximated by the analytic formula from Ref. 9:

$$T_{\mathbf{j} \times \mathbf{b}} = C \frac{\text{Im}[\Delta'_{\text{int}}(\Omega)]}{|-\Delta'_0 + \Delta'_{\text{int}}(\Omega)|^2} |\psi_{\text{vac}}|^2, \quad (8)$$

where  $C > 0$  is a geometrical factor independent of the plasma resistivity and rotation.  $\Delta'_0$  and  $\Delta'_{\text{int}}$  are the same as defined in Sec. IV. The lines in Fig. 8 represent the above analytic formula, applied for both vanishing and finite pressure cases. The analytic formula, Eq. (7), is used to evaluate  $\Delta'_{\text{int}}$ , and a least-square-fit to the plasma response field is used to calculate  $\Delta'_0$ , as described in Sec. V. We emphasize that, even though the above analytic formula (8) is derived for zero-pressure plasmas, it works well also for finite pressure cases. The only difference is to replace the pressure-less  $\Delta'_{\text{int}}$  (e.g., Eq. (29a) from Ref. 9) with the expression (7). The less satisfactory agreement between the MARS-F results and the analytic theory for the finite pressure case at faster rotation is due to the resonance of the finite frequency plasma response with continuum waves, which are not included into the analytic theory.

## VII. CONCLUSION AND DISCUSSION

We have reported an interesting physics effect of the screening of external fields by the resistive plasma response, at plasma rotation frequencies below  $\sim S^{-1/3} |D_R|^{2/3}$ , where  $S$  is the magnetic Lundquist number, and  $D_R$  is the resistive interchange index. This screening, due to the favorable average magnetic curvature effect on the tearing mode, is always associated with the finite pressure gradient at the rational surface.

For a simple toroidal equilibrium, we have demonstrated that the MARS-F computed plasma response to coil-generated external fields is well reproduced with the help of an analytic TM dispersion relation. Moreover, using the analytic dispersion relation, we can recover the tearing index from the computed plasma response. This offers an alternative approach of computing tearing index, which is a rather challenging task for toroidal plasmas with finite pressure gradient near rational surfaces.

Based on resistive MARS-F computations, we also find an enhanced toroidal coupling of the poloidal Fourier harmonics,

for the tearing mode eigenfunction in the resistive layer region, in the presence of the GGJ effect. The same effect also leads to the reversal of the sign of the toroidal electromagnetic torque, when an external static field is applied to a rotating resistive plasma with finite pressure. This sign reversal of the  $\mathbf{j} \times \mathbf{b}$  torque predicts the existence of a finite (but slow) steady state rotation even in the absence of a balancing viscous torque.

The screening effect associated with the GGJ-term occurs at very slow plasma flow ( $\sim 10^{-5} - 10^{-4} \omega_A$ ) for the large aspect ratio plasma considered in this work. On the other hand, typical toroidal flow speed observed in experiments ranges from a fraction of percent to several percent of the Alfvén speed. From this point of view, the results in this work are of more theoretical interest. However, there are at least two occasions where the GGJ-term induced screening can be of practical importance. The first is the RMP experiments with high plasma pressure, where the  $|D_R|$  value can be one order of magnitude larger than the case considered in this paper, and where the magnetic Lundquist number can be of order  $10^6$  or even lower, if we are primarily interested in the field screening near the plasma edge. The second occasion is the magnetic braking experiments, in which the plasma flow can be nearly fully damped. In the RMP case, the presence of the GGJ-screening does not necessarily prevent the field from penetrating into the plasma, since this can occur at a finite rotation. Also, other effects such as the electron diamagnetic flow, which is absent from the present single fluid model, may play a significant shielding role for the RMP field penetration.<sup>24</sup>

Some of the other effects reported in this work, e.g., the enhanced toroidal coupling and the strong amplification of the electromagnetic torque due to the GGJ effect, should be more generic.

## ACKNOWLEDGMENTS

This work was funded by the RCUK Energy Programme under Grant EP/I501045 and the European Communities under the contract of Association between EURATOM and CCFE. The views and opinions expressed herein do not necessarily reflect those of the European Commission.

<sup>1</sup>T. E. Evans, R. A. Moyer, K. H. Burrell, M. E. Fenstermacher, I. Joseph, A. W. Leonard, T. H. Osborne, G. D. Porter, M. J. Schaffer, P. B. Snyder, P. R. Thomas, J. G. Watkins, and W. P. West, *Nat. Phys.* **2**, 419 (2006).

<sup>2</sup>Y. Liang, H. R. Koslowski, P. R. Thomas, E. Nardon, B. Alper, P. Andrew, Y. Andrew, G. Arnoux, Y. Baranov, M. Boulet, M. Beurskens, T. Biewer, M. Bigi, K. Crombe, E. De La Luna, P. de Vries, W. Fundamenski, S. Gerasimov, C. Giroud, M. P. Gryaznevich, N. Hawkes, S. Hotchin, D. Howell, S. Jachmich, V. Kiptily, L. Moreira, V. Parail, S. D. Pinches, E. Rachlew, and O. Zimmermann, *Phys. Rev. Lett.* **98**, 265004 (2007).

<sup>3</sup>A. Kirk, Y. Q. Liu, E. Nardon, P. Tamain, P. Denner, P. Cahyna, I. Chapman, P. Denner, H. Meyer, S. Mordijck, D. Temple, and MAST Team, *Plasma Phys. Controlled Fusion* **53**, 065011 (2011).

<sup>4</sup>W. Suttrop, T. Eich, J. C. Fuchs, S. Guenter, A. Janzer, A. Herrmann, A. Kallenbach, P. T. Lang, T. Lunt, M. Maraschek, R. M. McDermott, A. Mlynek, T. Puetterich, M. Rott, T. Vierle, E. Wolfrum, Q. Yu, I. Zamamoto, and H. Zohm (ASDEX Upgrade Team), *Phys. Rev. Lett.* **106**, 225004 (2011).

<sup>5</sup>H. Reimerdes, J. Bialek, M. S. Chance, M. S. Chu, A. M. Garofalo, P. Gohil, Y. In, G. L. Jackson, R. J. Jayakumar, T. H. Jensen, J. S. Kim, R. J. La Haye,

- Y. Q. Liu, J. E. Menard, G. A. Navratil, M. Okabayashi, J. T. Scoville, E. J. Strait, D. D. Szymanski, and H. Takahashi, *Nucl. Fusion* **45**, 368 (2005).
- <sup>6</sup>M. P. Gryaznevich, T. C. Hender, D. F. Howell, C. D. Challis, H. R. Koslowski, S. Gerasimov, E. Joffrin, Y. Q. Liu, S. Saarelma, and JET-EFDA Contributors, *Plasma Phys. Controlled Fusion* **50**, 124030 (2008).
- <sup>7</sup>Y. In, M. S. Chu, G. L. Jackson, J. S. Kim, R. J. La Haye, Y. Q. Liu, L. Marrelli, M. Okabayashi, H. Reimerdes, and E. J. Strait, *Plasma Phys. Controlled Fusion* **52**, 104004 (2010).
- <sup>8</sup>R. Fitzpatrick and T. C. Hender, *Phys. Fluids B* **3**, 644 (1991).
- <sup>9</sup>R. Fitzpatrick, *Phys. Plasmas* **5**, 3325 (1998).
- <sup>10</sup>E. Nardon, P. Tamain, M. Bécoulet, G. Huysmans, and F. L. Waelbroeck, *Nucl. Fusion* **50**, 034002 (2010).
- <sup>11</sup>M. F. Heyn, I. B. Ivanov, S. V. Kasilov, W. Kernbichler, I. Joseph, R. A. Moyer, and A. M. Runov, *Nucl. Fusion* **48**, 024005 (2008).
- <sup>12</sup>Y. Q. Liu, A. Kirk, and E. Nardon, *Phys. Plasmas* **17**, 122502 (2010).
- <sup>13</sup>Y. Q. Liu, A. Kirk, Y. Gribov, M. P. Gryaznevich, T. C. Hender, and E. Nardon, *Nucl. Fusion* **51**, 083002 (2011).
- <sup>14</sup>A. H. Glasser, J. M. Greene, and J. L. Johnson, *Phys. Fluids* **18**, 875 (1975).
- <sup>15</sup>Y. Q. Liu, A. Bondeson, C. M. Fransson, B. Lennartson, and C. Breitholtz, *Phys. Plasmas* **7**, 3681 (2000).
- <sup>16</sup>B. Coppi, J. M. Greene, and J. L. Johnson, *Nucl. Fusion* **6**, 101 (1966).
- <sup>17</sup>A. H. Glasser, J. M. Greene, and J. L. Johnson, *Phys. Fluids* **19**, 567 (1976).
- <sup>18</sup>A. H. Glasser, S. C. Jardin, and G. Tesaro, *Phys. Fluids* **27**, 1225 (1984).
- <sup>19</sup>B. A. Carreras, H. R. Hicks, and D. K. Lee, *Phys. Fluids* **24**, 66 (1981).
- <sup>20</sup>T. C. Hender, R. J. Hastie, and D. C. Robinson, *Nucl. Fusion* **27**, 1389 (1987).
- <sup>21</sup>F. Militello, G. Huysmans, M. Ottaviani, and F. Porcelli, *Phys. Plasmas* **11**, 125 (2004).
- <sup>22</sup>C. J. Ham, Y. Q. Liu, J. W. Connor, S. C. Cowley, R. J. Hastie, T. C. Hender, and T. J. Martin, "Tearing stability in toroidal plasmas with shaped cross section," *Plasma Phys. Controlled Fusion* (submitted).
- <sup>23</sup>Y. Liu, *Comput. Phys. Commun.* **176**, 161 (2007).
- <sup>24</sup>F. L. Waelbroeck, *Phys. Plasmas* **10**, 4040 (2003).